

Contamination in LIB Pouch Cells Promoting Self-Discharge and Crosstalk

Robert Löwe^{*[a]} and Anna Smith^{*[a]}

Storage studies of lithium-ion battery electrolyte within bags made of commercial pouch foils, commonly used as encasing material of battery cells, revealed the presence of contamination leaching from the pouch foil material into the electrolyte. By analyzing the stored electrolyte via GC-MS the appearing compound was identified as 2,4-di-*tert*-butylphenol (2,4-DTBP). To investigate the influence of DTBP on the battery cell performance, full cells employing commercial LiNi_{1/3}Mn_{1/3}Co_{1/3}O₂ based cathodes and graphite-type anodes were assembled using 1 M LiPF₆ in ethylene carbonate/ dimethyl carbonate mixture as the electrolyte with/out the intentional addition of either 2,4-DTBP or its constitutional isomer 2,6-DTBP. Further-

more, dimethyl terephthalate (DMT), a literature known redox shuttle triggering impurity leaching from PET-based fixing tape used in LIBs, was added to compare the effect of DMT to DTBPs. It was revealed that either DTBP contaminations have a significant impact on the self-discharge behavior of the studied cells, which exceed the effect of present DMT. Moreover, all contaminants heavily increase transition metal dissolution-migration-deposition (TM DMD) processes and irreversible capacity loss. When vinylene carbonate, an SEI forming additive, is added to the electrolyte mixtures self-discharge, as well as TM DMD are suppressed to a different degree depending on the type of contaminant added.

Introduction

Aside from development regarding sustainability, safety and rate performance, another general goal of research in the field of lithium-ion batteries (LIB) is to increase their service life. Regardless of specific key performance indicators, the prevention of ageing and self-discharge of battery cells is a common goal for almost all applications and is therefore being investigated by many research groups.^[1–10] Recently, the redox shuttle active molecule dimethyl terephthalate (DMT) has attracted much attention, when it was identified as the monomer degradation product of the polymer polyethylene terephthalate (PET) tape that is used to hold the electrode stack in place.^[11] Replacing PET tape with polypropylene (PP) tape leads to an impressive reduction in self-discharge behavior of the cells studied.^[12] In any case, the authors demonstrate that DMT, once it appears within the battery cell, acts as a redox shuttle that significantly accelerates self-discharge.^[11–15]

Although the DMT-related self-discharge has received considerable attention, redox shuttle active molecules are not new to the field of battery research. In fact, this type of

functionality has been known and discussed in the literature for several decades as a favorable electrolyte additive to prevent cells from overcharging.^[16–25] Molecules that favor redox shuttle activities consist of an aromatic structure to which charge-stabilizing alkyl groups, such as *tert*-butyl groups, as well as alkoxy groups are attached. A small selection of overcharge protecting molecules discussed in literature are shown in Figure 1 in comparison to DMT. Although DMT does not have such charge-stabilizing alkyl groups with significant positive inductive effects, the extended aromatic π -system might sufficiently stabilize a charge during the shuttling process.

In addition to the fixation tape, other potential sources of unwanted contamination in lithium-ion battery cells are impurities or additives that can leach from inactive cell components such as the packaging, sealing/ gap filling and separator material. This work, specifically investigates the contamination introduced into the LIB cell by the use of commercial pouch foil as packaging material. State of the art pouch foils are typically a composite material consisting of the actual atmosphere barrier material, aluminum, and functional polymer layers on both sides of the aluminum foil. The outer polymer coating is multi-layered and includes PA and PET to provide electrical insulation and improve mechanical properties. In the form of cast polypropylene (CPP), PP is used as the inner layer within the pouch bag for the following purpose: 1) to protect the aluminum layer from electrolyte induced degradation/ corrosion, 2) to prevent short circuits due to its electronic insulating nature 3) to seal the inner pouch layer due to its low melting point allowing it to be formed into a bag in cell production.^[27,28] In state-of-the-art separators, again, PP is a major component together with polyethylene (PE).^[29] Although PP itself is recognized as a chemically stable material, polymer additives are necessary and commonly added to ensure oxidative stability during manufacture at elevated temper-

[a] R. Löwe, A. Smith

Institute for Applied Materials (IAM), Karlsruhe Institute of Technology, Hermann-Von-Helmholtz-Platz 1, D-76344 Eggenstein-Leopoldshafen, Germany

E-mail: Robert.Loewe@kit.edu
Anna.Smith@kit.edu

 Supporting information for this article is available on the WWW under <https://doi.org/10.1002/batt.202400368>

 © 2024 The Authors. Batteries & Supercaps published by Wiley-VCH GmbH. This is an open access article under the terms of the Creative Commons Attribution Non-Commercial NoDerivs License, which permits use and distribution in any medium, provided the original work is properly cited, the use is non-commercial and no modifications or adaptations are made.

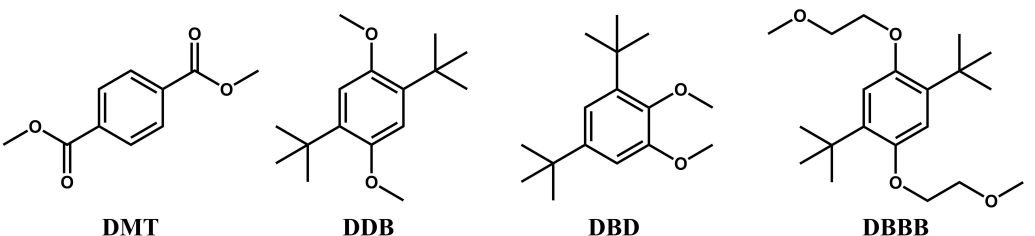


Figure 1. Chemical structure of dimethyl terephthalate (DMT) and exemplary structures of literature discussed overcharge protection additives, namely 2,5-di-*tert*-butyl-1,4-dimethoxybenzene (DDB)^[24]; 3,5-di-*tert*-butyl-1,2-dimethoxybenzene (DBD)^[26] and 2,5-di-*tert*-butyl-1,4-bis(2-methoxyethoxy)benzene (DBBB)^[25]

atures, to adjust mechanical properties and to provide long-term stability in use.^[30] A patent promoting the use of small sized metal oxide particles as additives in separator materials, briefly mentions that these particles could immobilize undesired impurities such as aromatic alcohols and fatty acids originating from the polymer feedstock of the PP separator.^[31] Antioxidants, which are often phenol and polyphenol derivatives, can be classified according to their ability to migrate.^[32] An extraction study by Haunschmidt et al. reveals the impressive variety of commercially used antioxidants and potential degradation products that can be released from PP samples.^[33] It appears that antioxidants commercially distributed under several trade names, e.g. Irganox™ and Irgafos™, as well as their degradation products 2,4-di-*tert*-butylphenol (2,4-DTBP)

and 4-*tert*-butylphenol (4-TBP) (see Figure 2) appear to have structural overlap with the previously discussed overcharging additives (see Figure 1). 2,6-Di-*tert*-butylphenol (2,6-DTBP) has been added to the list in Figure 2 as it is reasonable to assume that 2,6-DTBP derivatives could potentially occur as degradation products of antioxidants such as Irganox 1010 or PEP 36.

These polymer additives, which act as antioxidants, can have a significant effect on the cell chemistry and self-discharge characteristics of battery cells, if present. Therefore, this study investigates the effect of adding of either 2,4-, 2,6-DTBP, or DMT to the electrolyte of self-fabricated pouch cells using commercial LiNi_{1/3}Mn_{1/3}Co_{1/3}O₂ (NMC111) as the cathode and graphite as the anode material. The following results show that

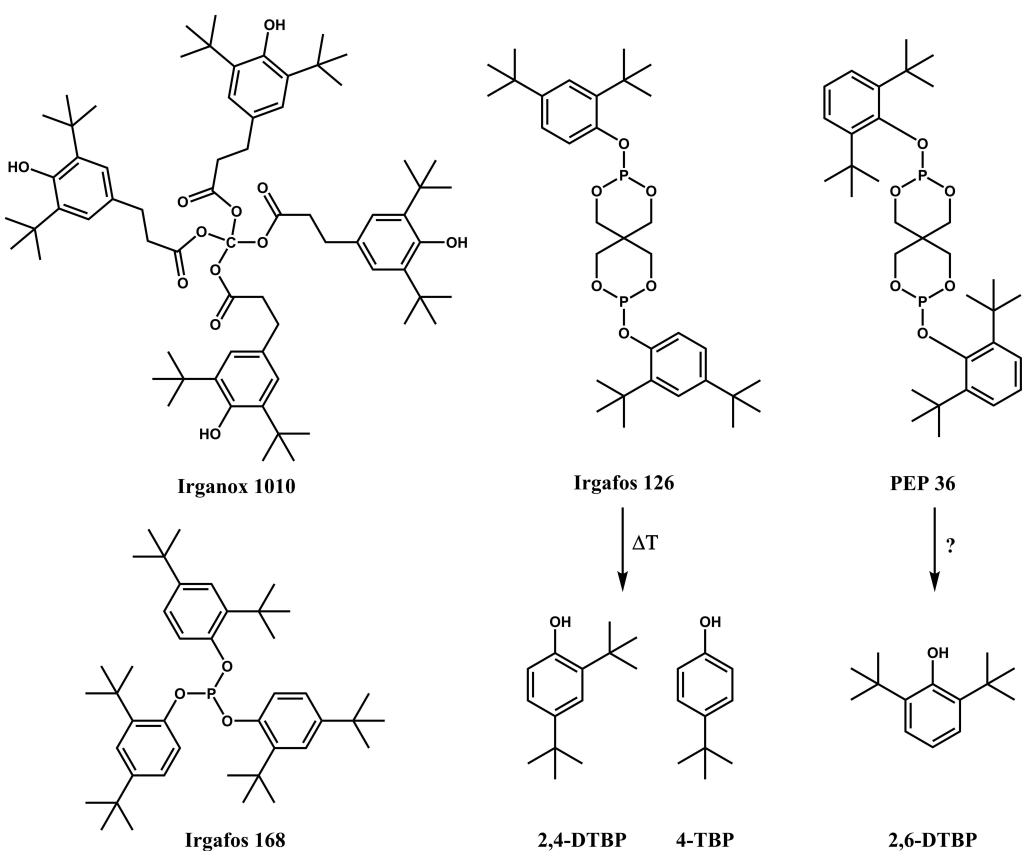


Figure 2. Exemplary chemical structures of literature known and extractable antioxidants from polypropylene (Irgafos, Irganox), PEP-type stabilizers, as well as possible degradation products 2,4-DTBP and 4-TBP^[33]. 2,6-DTBP was added to the list as a potential, but speculative degradation product.4

leaching of additives from inactive battery cell components should be of high concern.

Materials and Methods

Gas Chromatography–Mass Spectrometry (GC–MS)

Sample preparation of all GC–MS samples was carried out within a dry room (dew point $< -45^{\circ}\text{C}$). The pouch bags were cut open and 40 μL of the electrolyte were transferred into a small aluminum flask containing 1 mL of dichloromethane (DCM).^[38] Reference substances were dissolved in DCM to adjust the concentration to 1 wt.% in DCM. Before injection into the GC–MS instrument, the sample solutions were filtered through syringe filters. GC–MS experiments were carried out as described in literature.^[34,39] Those exact settings were used to obtain data displayed in Figure 3. These following settings were used to obtain data shown in Figure 4: A Clarus 690 GC from PerkinElmer (Waltham, USA) equipped with an Elite 5MS column (30 m length \times 0.25 mm interior diameter, 0.5 μm film thickness), an autosampler, a flame ionization detector (FID) and a MS detector (SQ 8 T) were used as measuring system. A continuous linear oven program from 40 $^{\circ}\text{C}$ to 300 $^{\circ}\text{C}$ was used, with a heating rate of 10 K/min and a holding time of 10 min at 300 $^{\circ}\text{C}$. The column pressure was adjusted to maintain a flow rate of 1.5 ml/min. The difference in retention times between Figure 3 and Figure 4 is mainly due to the adjustment of the oven program.

Inductively Coupled Plasma Optical Emission Spectroscopy (ICP–OES)

Prior to ICP–OES, the cells were discharged and held in CV phase at 3.0 V for 4 h to extract all mobile lithium-ions from the anode to the cathode. Afterwards, the cells were opened and carefully disassembled to prevent cross contamination of cathode materials onto the anode. The anodes were each washed with 10 mL DMC and dried for one hour. ICP–OES sample preparation and measurements were carried out by Dr. Thomas Bergfeldt in the group of

chemical analytic at KIT IAM-AWP. Weighed pieces of the anodes with a total weight of about 50–100 mg per electrode using a Mettler Toledo Inc. model XP56 (Columbus, USA). Anodes were subsequently put into aqua regia (6 ml hydrochloric acid subboiled and 2 ml nitric acid subboiled). The aqua regia with the electrodes was stored in a graphite oven (EasyDigest from Analab, Bischheim, France) at 80 $^{\circ}\text{C}$ for 4 h. An iCAP 7600 ICP–OES Duo (Thermo Fisher Scientific, USA) was employed to conduct quantitative analyses of lithium, manganese, nickel, and cobalt in electrodes. The quantification of these elements was achieved using four distinct matrix-adapted standard samples and the internal standard scandium. Scandium, added to each sample at a mass fraction of approximately 2.00 $\cdot 10^{-4}$ wt.%, facilitated the quantification process. The three primary wavelengths of each respective element were utilized for quantifying lithium, manganese, nickel, and cobalt.

Materials and Cell Manufacturing

2,4-DTBP (TraceCert), 2,6-DTBP (TraceCert) and DMT ($\geq 99\%$) were purchased from Merck (Switzerland). Single stack laboratory pouch cells (one cathode and one anode that are separated by one layer of separator) were assembled at the semi-automated battery production line at the Battery Technology Center at Karlsruhe Institute of Technology (KIT BATEC). Cells were built with calendered electrodes provided by a well-respected Korean supplier to meet industrial standards. Electrodes for all cells were single-sided coated with LiNi_{0.33}Mn_{0.33}Co_{0.33}O₂ (NMC111) as cathode active material and graphite as anode active material. The separator consists of a non-woven PET structure in which alumina particles are embedded. Stock electrolytes are 1 M LiPF₆ in EC:DMC (weight ratio 1:1) provided by BASF (Ludwigshafen, Germany) and 1 M LiPF₆ in EC:DMC (weight ratio 1:1) including 3 wt% of VC, provided by E-Lyte Innovations (Kaiserslautern, Germany), henceforth referred to as LP30 and LP30 + 3 wt% VC, respectively. For a detailed description of the manufacturing process and electrode characteristics it is referred to a previous publication.^[35] For the following results it might be important to mention that the electrolyte filled cells were kept at 25 $^{\circ}\text{C}$ for assembly, testing and post-mortem

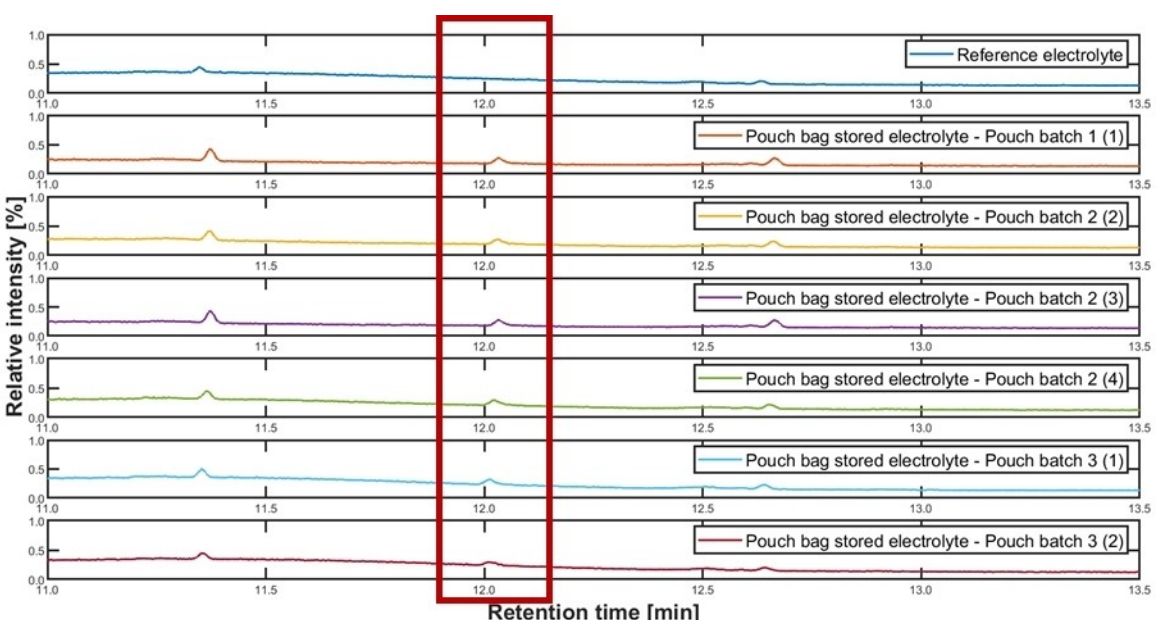


Figure 3. Enlargement of GC chromatograms between 11.0 min and 13.5 min retention time showing the presence of a contamination (at 12.0 min) within the electrolyte during a 10 weeks storage period at 60 $^{\circ}\text{C}$ in pouch bags.

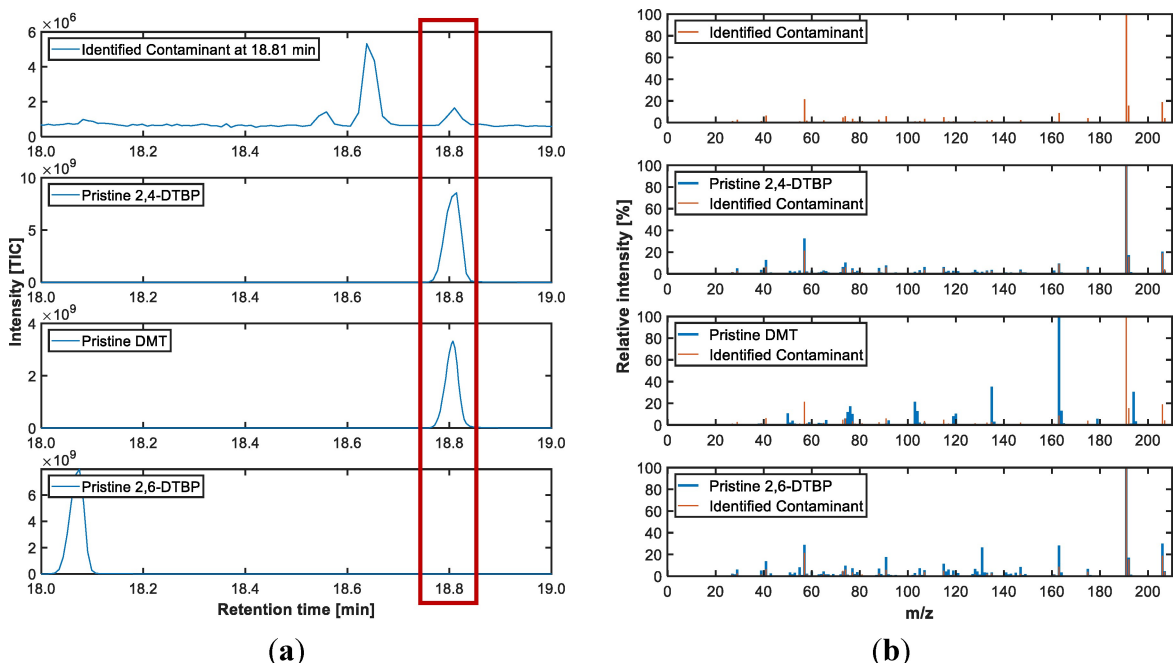


Figure 4. (a) Comparison of GC chromatograms in terms of retention time for the electrolyte sample stored in the pouch bag, 2,4-DTBP, DMT and 2,6-DTBP, all diluted in dichloromethane; (b) MS fragmentation patterns of eluting compounds (top panel: contaminant at $t = 18.8$ min, 2nd panel: 2,4-DTBP at 18.8 min., 3rd panel: DMT at 18.8 min. and 4th panel with 2,6-DTBP at 18.1 min.), 2nd-4th panels include an overlay of the MS fragmentation pattern of the contaminant eluting at 18.8 min.

procedures, except for a 24 h wetting period at 40 °C, prior to cell formation.

Cell testing and Formation

The battery cells were tested on BaSyTec CTS LAB instruments while they were placed inside a climatic chamber at 25 ± 0.1 °C. All cell tests were performed in a voltage window between 3.0 V and 4.2 V. Cell formation was carried out applying an initial C/10 charging, followed by C/2 discharge and five subsequent C/2 charge/discharge cycles. Unless otherwise stated, within all cell tests, charging was performed in a CC-CV mode until $I < C/20$ at 4.2 V in CV-phase. Discharge was performed in CC mode to 3.0 V. The test protocol designed for the self-discharge test and ir/reversible capacity determination is described in the results section. Within the check-up procedure, the state-of-charge (SoCs) were adjusted in charge direction by Ah counting for internal DC resistance (RiDC) and open circuit voltage (OCV) determination. RiDC values were determined by applying a single 1 C discharge pulse for 20 seconds at certain SoC. Applying Ohm's law, the DC internal resistances were determined using the potential drop (difference between the potential at the end of the pulse and the potential in rest state before the pulse) and the applied current for the respective pulses. OCV readings were taken from the last OCV voltage relaxation reading 30 min. after SoC adjustment prior to pulsing.

Results and Discussion

Identification of Pouch Foil Introduced Contaminations in LIB Cells

The initial objective was to determine the electrolyte stability of different batches of pouch foil, which were deep drawn under varying parameters. Prepared pouch bags, see Figure S1, were filled with a commercial electrolyte containing 1 M LiPF₆ in a mixture of EC, DMC, and EMC to which 500 ppm water was added. The addition of water was intended to simulate residual moisture that is generated *in situ* or introduced into the pouch bag during cell production e.g., due to residual moisture of various cell components.^[36,37] Following electrolyte filling, the pouch bags were sealed under reduced pressure and stored in a climate chamber at 60 °C for ten weeks. After ten weeks, the bags were opened and analyzed. Visual inspection of the interior showed that the pouch bags were intact for all material batches and deep drawing parameters. At first glance, the GC chromatograms of the electrolyte samples compared with a reference electrolyte showed no unexpected differences (see Figure S2). However, more detailed analysis revealed the occurrence of a component eluting at 12.0 min from pouch bag stored electrolyte samples that was not found in the reference electrolyte (see Figure 3). Two potential sources of contamination were identified: i) the inside of the pouch material, which consists of PP and ii) the outside of the pouch material, which consists of PET. The background to the latter is that pouch foils are delivered and stored on rolls. Therefore, during storage, the

inside and outside of the pouch material are in direct contact and could potentially contaminate each other.

To identify the compound eluting at 12.0 min, its MS fragmentation pattern was compared with the NIST (National Institute of Standards and Technology, U.S. Department of Commerce) database resulting in a high match with di-*tert*-butylphenol, specifically either 2,4-DTBP or 2,6-DTBP. To validate the experimental retention time and for sake of completeness, samples of pure 2,4-DTBP, 2,6-DTBP and also DMT, the previously identified PET degradation product, were prepared for GC-MS analysis. At this point, the GC column and temperature program were modified for further analyses. Consequently, the retention time of the impurity shifted from 12.0 to 18.8 min. The GC chromatograms and MS spectra of the pure reference substances were compared with the contaminant in terms of retention time and MS fragmentation pattern, respectively, see Figure 4.

Based on the retention time and MS fragmentation pattern, 2,4-DTBP was clearly assigned to the contaminant found, whereas 2,6-DTBP could be excluded because neither retention time, nor MS fragmentation was consistent with the impurity. The most striking difference in the MS fragmentation pattern between the two DTBP isomers is a fragment at $m/z = 131$ which is very prominent for 2,6-DTBP, but of low relative intensity for 2,4-DTBP and the contaminant studied. Furthermore, it was found that the difference in retention time between DMT and 2,4-DTBP during reference measurements was negligible ($\Delta t < 0.02$ min), thus making them indistinguishable. Despite similar retention times (see Figure 4 a), correct assignment was possible by MS fragmentation (see Figure 4 b, and also see Figure S3–6 for magnification of individual panels of Figure 4 b). In the case of the identification of DMT, which acts as a redox shuttle molecule, described in the literature a matching retention time was stated as a main argument for the identification of DMT.^[11] Although the similarity in the retention time of DMT and 2,4-DTBP determined in this study may be a coincidence using our specific GC-MS settings, there is a possibility that 2,4-DTBP was also present in the cells described in the literature.^[11,13,14]

Setup of the Battery Cell Testing Conditions

Single-layer laboratory pouch cells based on NMC111 cathodes and graphite anodes were assembled with different electrolyte compositions as shown in Table 1. For that purpose, the stock electrolytes used were either LP30 or LP30 including 3 wt.% vinylene carbonate (VC) as an SEI-forming additive. The following contaminants in question were deliberately added at concentrations of either 1 or 2 wt.%; 2,4-DTBP was identified as a contaminant in the pouch bags, so its influence on the electrochemical properties of a full battery cell had to be investigated. In addition, it was of great interest to study whether the position of the *tert*-butyl group had an influence on the electrochemical properties of a battery cell. Therefore, 2,6-DTBP was used in comparison to 2,4-DTBP. Furthermore, the effect of the addition of DMT, the previously identified redox-shuttle, is also studied in direct comparison to DTBPs.

All cell tests, including formation, were performed at 25 °C. The test routine was derived from that used by Büchele et al. used in their studies on the influence of DMT, but modified in certain respects.^[14] Figure 5 illustrates the test routine used in this study. The derived test includes a more detailed cell characterization via check-ups, applied before and after a 500 h lasting OCV phase, embedded in a C/4 charge/ discharge cycle. The check-up procedure includes two 1 C charge/ discharge cycles to compare the capacity retained at a higher load to C/4, and state-of-charge (SoC) dependent OCV readings, as well as internal resistance measurements (RiDCs), which provide in-depth insight into the shift of SoC dependent OCV values and internal resistances, respectively.

Initial C/4 discharge capacities (D_{init}) were measured after formation prior to testing. The ir/reversible capacity loss data shown in the following section has been determined from the C/4 cycle discharge capacities. More specifically, the overall capacity loss during the storage period ($D_0 - D_1$) is the sum of all reversible and irreversible capacity losses. The irreversible calendric capacity loss is the difference between the discharge capacities of C/4 cycles before and after the storage containing cycle ($D_0 - D_2$). The reversible capacity loss is defined by $(D_0 - D_1) - (D_0 - D_2)$.^[40]

Table 1. Overview of electrolyte variations with intentionally added contaminants used in the cells studied.

Stock electrolyte	Intentionally added contaminant	Stock electrolyte	Intentionally added contaminant
LP30 (1 M LiPF ₆ in EC/DMC with weight ratio 1:1)	–	LP30 + 3 wt.% VC (LP30 + VC with weight ratio 97:3)	–
	1 wt.% 2,4-DTBP		1 wt.% 2,4-DTBP
	2 wt.% 2,4-DTBP		2 wt.% 2,4-DTBP
	1 wt.% 2,6-DTBP		1 wt.% 2,6-DTBP
	2 wt.% 2,6-DTBP		2 wt.% 2,6-DTBP
	1 wt.% DMT		1 wt.% DMT
	2 wt.% DMT		2 wt.% DMT

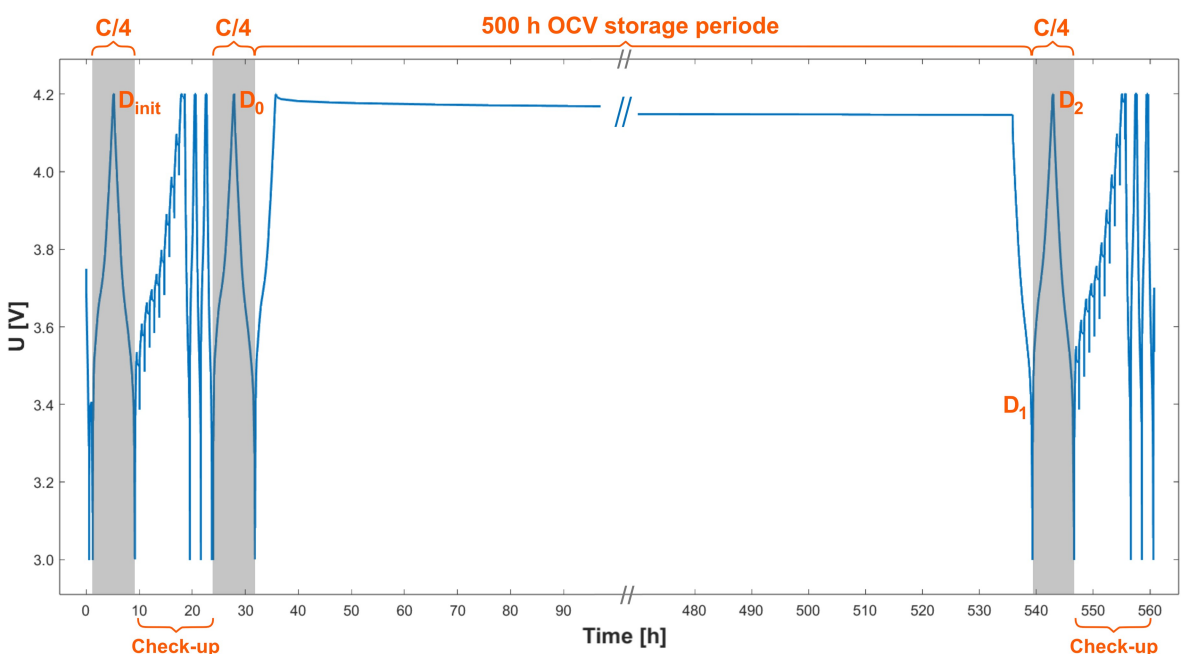


Figure 5. Time-dependent voltage curve exemplarily illustrating the testing protocol used in this study to evaluate self-discharge and Ir/reversible capacity loss. D always refers to the corresponding discharge capacity.

Influence of DTBP and DMT on Lithium-Ion Battery Self-Discharge and Ir/Reversible Capacity Loss

It was found that the intentionally added 2,4-DTBP, 2,6-DTBP and the literature known redox shuttle molecule DMT significantly influence the self-discharge behavior. Over the 500 hour lasting storage period at 25 °C, the decrease in recorded OCV values varies greatly depending on the added contaminant and its concentration (see Figure 5 a and Figure 6 b). The OCV drop during storage for the same added substance increases with increasing concentration. For both concentrations studied, added to either one of the stock electrolytes (with/without VC additive) 2,6-DTBP causes the most pronounced OCV drop and thus self-discharge. Comparing the OCV curve shapes of 2,4-DTBP and DMT contaminated cells without VC as additional additive in Figure 6 a, it appears that 2,4-DTBP induces a higher initial OCV drop than DMT during the first 100 hours of storage. While the voltage curves flatten over time for 2,4-DTBP containing cells, they are almost linear for DMT containing cells. It can be assumed that different electro/chemical mechanisms are causal for the observed OCV reductions. In the case of cells built with VC as an SEI-forming additive, the corresponding DMT-containing cells also show a flattening of the OCV curves over time (see Figure 6 b). Overall, it seems likely, that the added contaminants strongly interfere with the SEI formation process/ composition, as the addition of VC generally reduces the OCV drop, but also changes the curve shapes in the case of DMT addition. However, detailed investigations are needed to shed more light on the exact mechanisms but are beyond the scope of this work.

The OCV-SoC dependence remains constant before and after the storage period for most of the electrolyte variations

studied (see Figure 6 c and d). Therefore, drastic changes in the electrode chemistry can be excluded as the main reason for the OCV reduction. However, there are changes in the SoC vs. OCV curves for cells with 2 wt.% 2,6-DTBP in LP30 and 2 wt.% DMT in LP30 + VC. Although such high concentrations of contaminants are unlikely to occur in common cells, it is another indication that non-self-discharge related ageing mechanisms may be triggered by these classes of contaminants.

When comparing the C/4 discharge capacities (D_{init}) of the fresh cells, it is noticeable that the addition of the studied contaminants already reduces the initial cell capacity even before the storage period is applied (see Figure 7a, b). This effect is more pronounced at higher contaminant concentrations. It should be noted that the presence of VC results in lower initial capacities (~2 mAh). The influence on the initial cell capacity after formation is another indicator that the contaminations somehow influence the SEI e.g., by suppressing the SEI formation to a certain level. Furthermore, the addition of the studied contaminants leads to a significant increase in self-discharge during the 500 h storage period at room temperature (see Figure 7 a, b). Ir/reversible losses are also shown as relative values in Figure 7 c, d. For both stock electrolytes, 2,6-DTBP leads to higher total capacity losses than 2,4-DTBP. Higher contaminant concentrations increase the self-discharge, which is consistent with the observed corresponding OCV reductions. However, in the presence of VC, the total capacity loss is reduced as indicated by the lower decrease in OCV/ SoC over storage of 500 h. In general, a higher SoC of the battery cell should result in an overall increase in calendrical ageing, e.g. due to electrolyte degradation, which is seen as increased absolute irreversible capacities when VC is present. Interestingly, 2,6-DTBP in LP30 causes the highest irreversible losses

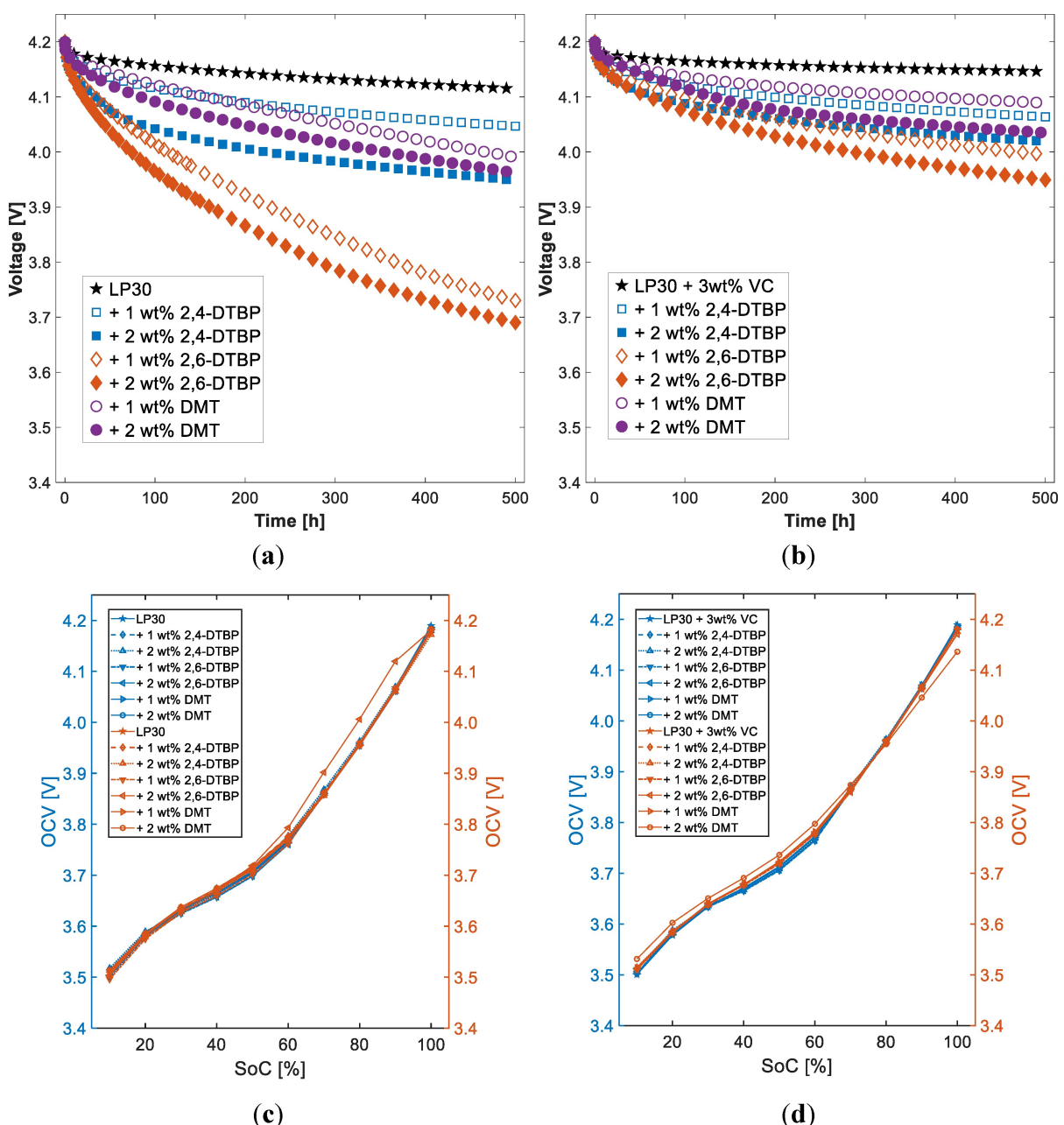


Figure 6. Open-circuit voltage curve over time during the 500 h lasting storage period for cells with (a) LP30 as stock electrolyte; (b) LP30 + 3 wt % VC as stock electrolyte. For the sake of legibility only every third measured data point is plotted. OCV vs. SoC curves from check-up cycles before (blue) and after (orange) the 500 h lasting storage period for cells with (c) LP30 as stock electrolyte; (d) LP30 + 3 wt % VC as stock electrolyte.

even though the final SoC of the cell is lowest at ~50%, whereas e.g. DMT resulted in a reduction of the SoC to 80% but lower irreversible capacity loss. DMT containing electrolyte caused highest irreversible capacity losses in LP30 + VC electrolyte. Overall, all coulombic efficiencies (CE) for 1 C and C/4 cycles were in the range of 100%, meaning that no significant charge loss is observed due to subsequent discharge after charging, regardless of the electrolyte composition.

In Figure 8 RiDC values during the check-up procedures are compared before and after the storage period. As would be expected, due to cell ageing, which should correlate directly with irreversible capacity loss, there is a general trend for RiDC

values to increase after the storage period. However, there are certain deviations from this trend. For most cells, including the reference cells, the RiDC values before the storage period are relatively high at SoC 10–20% and are in many cases even higher than after the storage. It can be observed that the addition of 2,6-DTBP causes significantly higher increases in RiDCs compared to the other contaminants in LP30, which is in line with the above discussed highest irreversible capacity loss induced by this contaminant. In the presence of VC, all RiDC values are slightly higher than without VC, especially after the storage period, and in line with the irreversible capacity losses discussed above, DMT induces greater increase in RiDC values

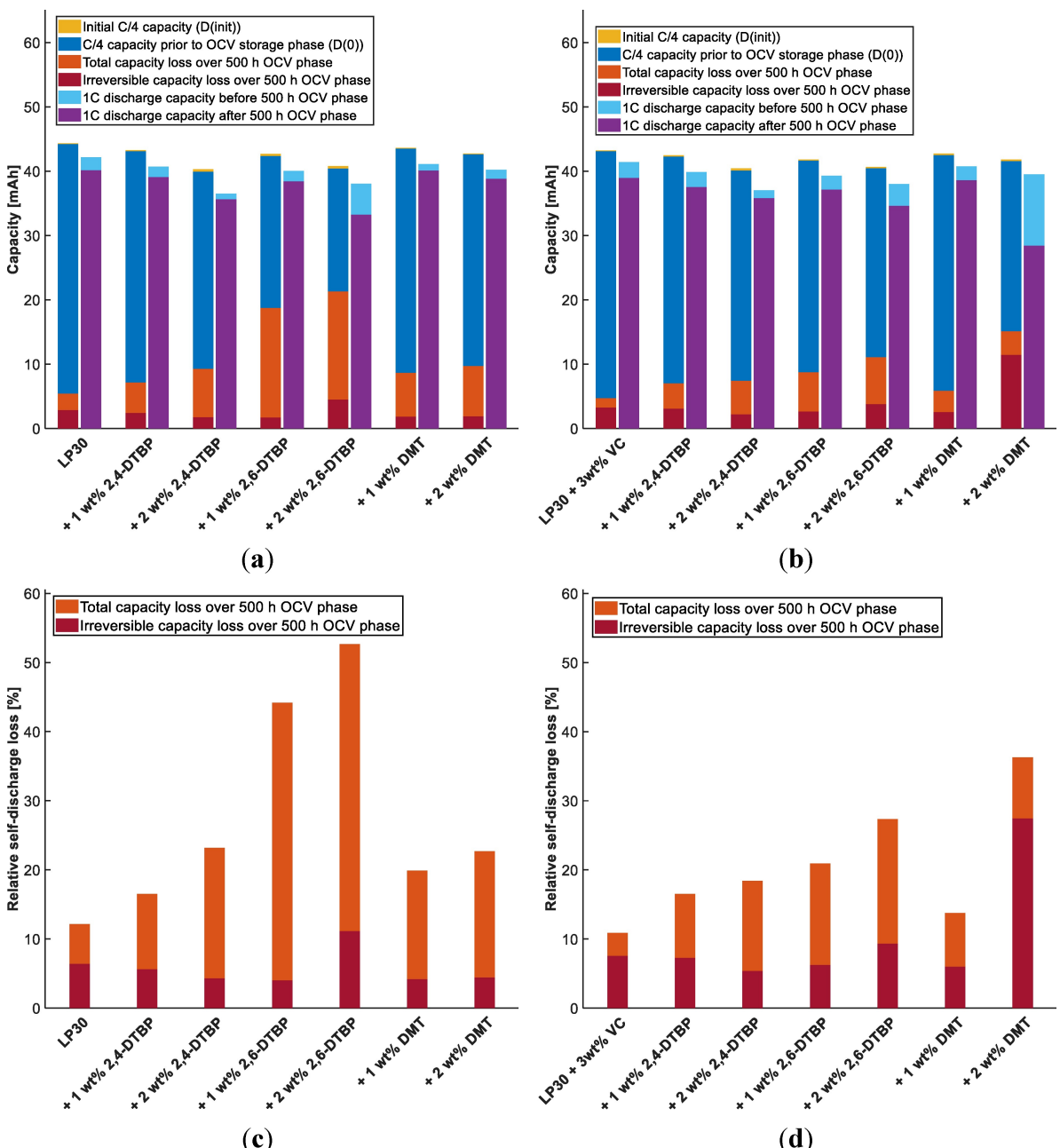


Figure 7. Bar graphs of the absolute discharge capacity [mAh] measured at C/4 before the storage period of 500 hours overlaid with the total capacity loss (sum of reversible and irreversible loss) and the irreversible capacity loss during storage period for (a) cells with LP30 as stock electrolyte; (b) cells with LP30 + 3 wt.% VC as stock electrolyte. Relative storage discharge capacity loss overlaid with irreversible storage capacity loss for cells with c) LP30 as stock electrolyte; (d) LP30 + 3 wt.% VC as stock electrolyte.

in the VC-containing electrolyte. Again, these observations suggest that the contaminants investigated are not just transporting charges in a trivial way, but are acting in a more complex manner and may be interfering with the cell chemistry.

It has been described in literature that transition metal dissolution-migration-deposition (TM DMD) processes are associated with both SEI appearance and capacity fading. Briefly, transition metals such as manganese that are deposited on the anode's SEI can lead to a catalytic cycle of electrolyte

decomposing and irreversible trapping of lithium-ions in the SEI, which reduces the cell capacity.^[41–43] Since the added contaminants reduce the initial cell capacity and also appear to interfere with the SEI, the amounts of anode-deposited TM were quantified via ICP-OES. The results (see Table 2 and Figure 9) show that both, DTBPs and DMT act not only as self-discharging agents, but also as TM DMD promoting agents. The contaminants increase anodic TM deposition in the order DMT < 2,4-DTBP ≤ 2,6-DTBP. With VC as an additive all TM values are slightly lower compared to VC-free electrolytes. The amount of

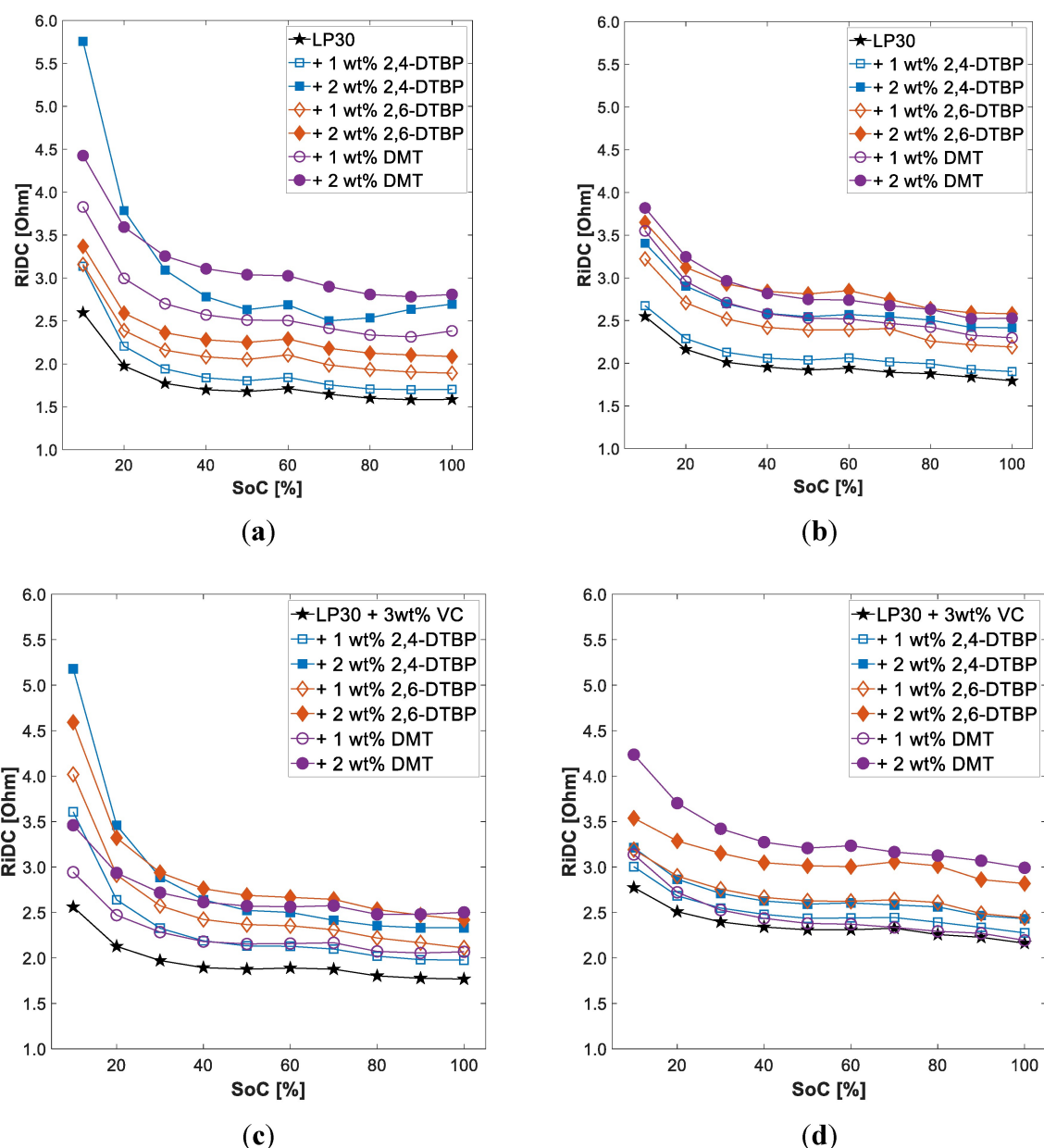


Figure 8. RiDC values at studied SoCs with LP30 as stock electrolyte (a) before and (b) after 500 h storage. RiDC values at studied SoCs with LP30 + 3 wt.% VC as stock electrolyte (c) before and (d) after 500 h storage.

TMs deposited does not seem to correlate with the irreversible capacity loss, e.g. DMT showed the highest irreversible capacity loss in LP30 + VC, but rather low TM deposition. Note that anodes of VC-containing electrolyte also show more irreversible lithium trapped (Figure S7), which is consistent with the higher capacity loss of VC-containing battery cells.

Before TMs can be deposited on the anode, the respective TM must be dissolved from the cathode side and transported through the electrolyte to the anode. It is very likely that the studied contaminants accelerate this process, perhaps as highly soluble TM-carrying complexes. Overall, the addition of VC as an SEI-forming agent, reduces the amount of TM deposited on the anode side. Two hypothetical explanations for this observation are: i) the differently composed SEI formed in the presence

of VC reduces the TM deposition; ii) the SEI reduces an electrochemical activation process that the contaminants must undergo to allow TM dissolution from the cathode and/or TM transport. The latter would complement the self-discharge mechanism of DMT described in the literature, which also correlates with an electrochemical activation process at the anode.^[13,15] A third explanation, including the deactivation of the contaminants by direct reactions with VC seems unlikely from a molecular perspective and would not explain the significant TM DMD within the VC-containing cells.

Data from the cell testing and ICP-OES lead to the conclusion that both, DTBPs and DMT cause several complex mechanisms leading to self-discharge, transition metal deposition on the anode and irreversible capacity loss. Comparing all

Table 2. Quantification of lithium, nickel, cobalt, and manganese by ICP-OES on the anode of *post-mortem* opened cells after the conducted cell testing. Values are expressed as wt.% of the total anode (including copper foil and coating).

Material/Electrolyte	Lithium	Manganese	Cobalt	Nickel
Pristine anode	-	-	-	-
LP30	0.411	0.002	0.001	0.002
LP30 + 2 wt.% 2,4-DTBP	0.487	0.010	0.008	0.010
LP30 + 2 wt.% 2,6-DTBP	0.475	0.015	0.008	0.011
LP30 + 2 wt.% DMT	0.426	0.004	0.002	0.003
LP30 + 3 wt.% VC	0.530	0.001	0.001	0.001
LP30 + 3 wt.% VC + 2 wt.% 2,4-DTBP	0.523	0.008	0.005	0.007
LP30 + 3 wt.% VC + 2 wt.% 2,6-DTBP	0.589	0.012	0.004	0.007
LP30 + 3 wt.% VC + 2 wt.% DMT	0.511	0.002	0.001	0.002

the results, it is clear that the position of the *tert*-butyl groups in DTBP has a significant influence on the electrochemical effect in the battery cell. 2,4-DTBP results in only 50% of the amount of self-discharge induced by 2,6-DTBP. 2,4-DTBP has less effect on TM DMD for manganese and nickel than 2,6-DTBP. However, 2,4-DTBP induces even higher anode deposition of manganese than 2,6-DTBP. Overall, the effect of the substitution pattern is much less pronounced for TM DMD than for the self-discharge behavior. Although the addition of DMT and 2,4-DTBP to the electrolyte leads to comparable self-discharge over 500 h storage, DMT induces far less TM DMD than 2,4-DTBP. This strengthens the hypothesis that a complex system of multiple

overlapping mechanisms is causal for the observed self-discharge and TM DMD behavior. The strong manifestation of these phenomena after only approximately one month cell lifetime at room temperature between electrolyte filling and *post-mortem* analysis indicates that contaminations like 2,4-DTBP could be concerning contaminations that promote self-discharge and TM DMD, and irreversible capacity loss in lithium-ion battery cells.

Conclusions

2,4-Di-*tert*-butylphenol released from the pouch cell casing was identified as a battery cell contaminant of concern. A literature research provided a reasonable explanation for the origin of this observation. Antioxidants used in PP carrying the 2,4-DTBP or similar structures may degrade or react with the electrolyte releasing these types of phenol derivatives. Both 2,4-DTBP and 2,6-DTBP are structurally similar to known redox shuttle active molecules that have been discussed in the literature as overcharge protection additives for battery electrolytes. Indeed, 2,4-DTBP and 2,6-DTBP were found to promote self-discharge of the cells studied. Yet, they also affect the battery chemistry through unfavorable effects, which are more pronounced with the addition of the 2,6- derivative than the 2,4-derivative, showing that the substitution pattern plays a significant role in this context. These effects were directly compared with another recently described contaminant, DMT. Several indicators suggest that both DTBPs and DMT affect the cell chemistry through more complex phenomena than just charge transfer. It was found that irreversible capacity loss and transition metal deposition on the anode is increased when the studied

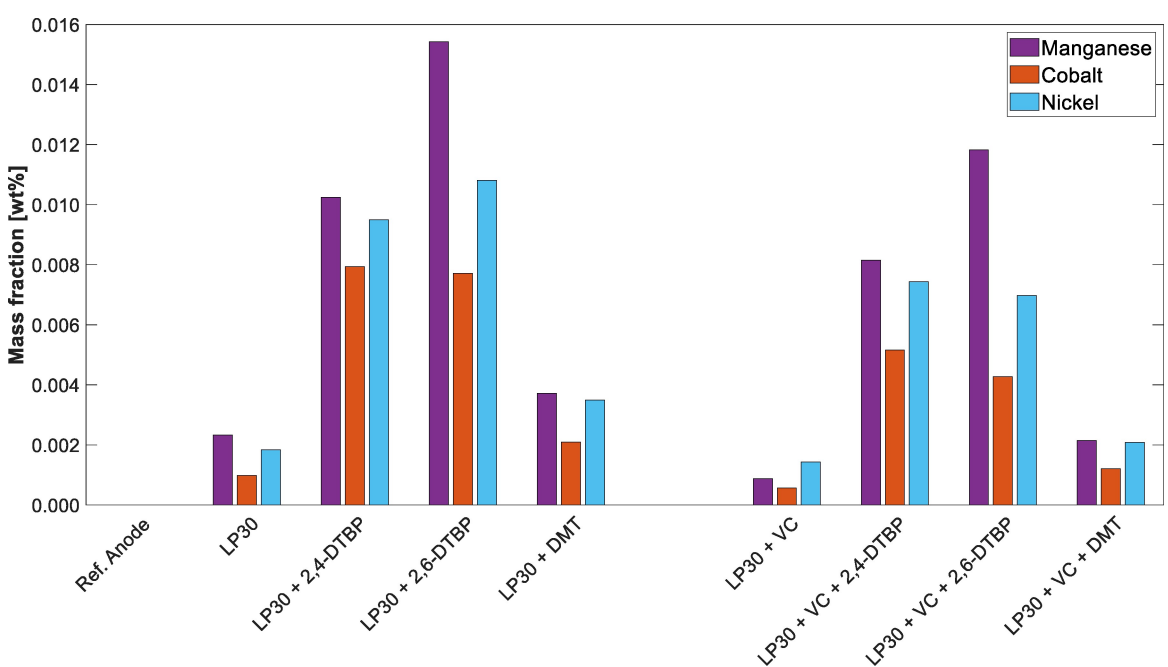


Figure 9. ICP-OES determined mass fractions of the transition metals manganese, cobalt, and nickel in the anode of *post-mortem* opened cells after the self-discharge test was applied. In addition to a pristine anode and the studied reference cells, only cells containing 2 wt.% of contaminants were analyzed.

molecules were added to the electrolyte. Both effects, increased self-discharge and TM DMD caused by the studied molecules, can be partly suppressed by addition of VC as an SEI forming additive. This correlation clearly shows that the forming SEI characteristics are related to the contaminants added to the electrolyte. Further studies addressing the mechanism responsible for self-discharge, TM dissolution, their migration through the electrolyte, irreversible capacity loss, as well as interplay with the SEI will be objective of following research activities. It is concluded that the use of extractable polymer additives needs to be given more attention, especially by polymer manufacturers for battery applications, in order to improve battery cell longevity. Intuitively, non-migratory antioxidants that are covalently bound to the polymer backbone should be preferred in battery materials as they have a lower probability of leaching into the electrolyte and thus contaminating the battery cell electrolyte.

Funding

The authors express their gratitude for the financial support. This research was part of the project "PaXibel" within the research initiative "Battery Materials for Future Mobile and Stationary Applications – Battery 2020" and funded by the German Federal Ministry of Education and Research under the grant number "03XP0400E". This work contributes to the research performed at CELEST (Center for Electrochemical Energy Storage Ulm & Karlsruhe), and was done at the KIT Battery Technology Center (KIT-BATEC).

Author Contributions

Conceptualization, R.L.; methodology, R.L.; investigation, R.L.; resources, A.S.; data curation, R.L.; writing–original draft preparation, R.L.; writing–review and editing, R.L. and A.S.; visualization, R.L.; funding acquisition, A.S. All authors have read and agreed to the published version of the manuscript.

Acknowledgements

We would like to thank Karsten Schmidt, Sven Leuthner and Olivia Wiegand for assembly of the pouch cells. Also greatly acknowledged are GC-MS measurements conducted by Dr. Freya Janina Müller and Dr. Andreas Hofmann. We further thank Dr. Thomas Bergfeldt for carrying out the sample preparation and ICP-OES measurements. We would also like to thank Nils Schmidgruber (KIT wbk) for initiating of the PaXibel project. Open Access funding enabled and organized by Projekt DEAL.

Conflict of Interests

The authors declare no conflict of interest.

Data Availability Statement

The data that support the findings of this study are available in the supplementary material of this article.

Keywords: Lithium-ion batteries · Self-discharge · Redox shuttle molecule · Transition metal dissolution-migration-deposition (TM DMD) · Electrolyte contamination

- [1] A. Ghamlouche, M. Müller, F. Jeschull, J. Maibach, *J. Electrochem. Soc.* **2022**, *169*, 20541, DOI 10.1149/1945-7111/ac4cd3.
- [2] C. Xu, et al., *Nature materials* **2021**, *20*, 84–92, DOI 10.1038/s41563-020-0767-8.
- [3] I. Buchberger, et al., *J. Electrochem. Soc.* **2015**, *162*, A2737–A2746, DOI 10.1149/2.0721514jes.
- [4] Z. Ruff, C. Xu, C. P. Grey, *J. Electrochem. Soc.* **2021**, *168*, 60518, DOI 10.1149/1945-7111/ac0359.
- [5] X. Yan, et al., *ACS Energy Lett.* **2023**, *8*, 2376–2384, DOI 10.1021/acsenergylett.3c00453.
- [6] W. M. Seong, et al., *Energy Environ. Sci.* **2018**, *11*, 970–978, DOI 10.1039/C8EE00186C.
- [7] S. E. Sloop, J. B. Kerr, K. Kinoshita, *J. Power Sour.* **2003**, *119*–*121*, 330–337, DOI 10.1016/S0378-7753(03)00149-6.
- [8] T. Utsunomiya, O. Hatozaki, N. Yoshimoto, M. Egashira, M. Morita, *J. Power Sour.* **2011**, *196*, 8598–8603, DOI 10.1016/j.jpowsour.2011.05.066.
- [9] A. Blyr, et al., *J. Electrochem. Soc.* **1998**, *145*, 194–209, DOI 10.1149/1.1838235.
- [10] R. YAZAMI, Y. REYNIER, *Electrochim. Acta* **2002**, *47*, 1217–1223, DOI 10.1016/S0013-4686(01)00827-1.
- [11] S. Buechele, et al., *J. Electrochem. Soc.* **2023**, *170*, 10511, DOI 10.1149/1945-7111/acaf44.
- [12] A. Adamson, et al., *Nature Mater.* **2023**, DOI 10.1038/s41563-023-01673-3.
- [13] T. Boulanger, et al., *J. Electrochem. Soc.* **2022**, *169*, 40518, DOI 10.1149/1945-7111/ac62c6.
- [14] S. Buechele, et al., *J. Electrochem. Soc.* **2023**, *170*, 10518, DOI 10.1149/1945-7111/acb10c.
- [15] T. Boetticher, A. Adamson, S. Buechele, E. D. Alter, M. Metzger, *J. Electrochem. Soc.* **2023**, *170*, 60507, DOI 10.1149/1945-7111/acd8fd.
- [16] J. Zhang, et al., *Materials Today Energy* **2019**, *13*, 308–311, DOI 10.1016/j.mtener.2019.06.003.
- [17] W. K. Behl, Chin, *J. Electrochem. Soc.* **1988**, *135*, 16–21, DOI 10.1149/1.2095545.
- [18] L. M. Moshurchak, et al., *J. Electrochem. Soc.* **2009**, *156*, A309, DOI 10.1149/1.3077578.
- [19] R. S. Assary, L. Zhang, J. Huang, L. A. Curtiss, *J. Phys. Chem. C* **2016**, *120*, 14531–14538, DOI 10.1021/acs.jpcc.6b04263.
- [20] Z. Chen, Q. Wang, K. Amine, *J. Electrochem. Soc.* **2006**, *153*, A2215, DOI 10.1149/1.2352048.
- [21] W. Weng, J. Huang, I. A. Shkrob, L. Zhang, Z. Zhang, *Adv. Energy Mater.* **2016**, *6*, DOI 10.1002/aenm.201600795.
- [22] L. Zhang, Z. Zhang, K. Amine, *ECS Trans.* **2013**, *45*, 57–66, DOI 10.1149/04529.0057ecst.
- [23] J. Zhang, et al., *Journal of Power Sources* **2018**, *378*, 264–267, DOI 10.1016/j.jpowsour.2017.12.059.
- [24] C. Buhrmester, et al., *J. Electrochem. Soc.* **2005**, *152*, A2390, DOI 10.1149/1.2098265.
- [25] L. Zhang, Z. Zhang, P. C. Redfern, L. A. Curtiss, K. Amine, *Energy Environ. Sci.* **2012**, *5*, 8204, DOI 10.1039/c2ee21977h.
- [26] J. K. Feng, X. P. Ai, Y. L. Cao, H. X. Yang, *Electrochemistry Communications* **2007**, *9*, 25–30, DOI 10.1016/j.elecom.2006.08.033.
- [27] B. K. Park, et al., *J. Power Sour.* **2021**, *506*, 230222, DOI 10.1016/j.jpowsour.2021.230222.
- [28] Z. Guo, Y. Fan, *RSC Adv.* **2016**, *6*, 8971–8979, DOI 10.1039/C5RA27097A.
- [29] V. Deimedé, C. Elmasides, *Energy Tech.* **2015**, *3*, 453–468, DOI 10.1002/ente.201402215.
- [30] V. Marturano, P. Cerruti, V. Ambrogi, *Polym. Addit. Phys. Sci. Rev.* **2017** *2*, DOI 10.1515/psr-2016-0130.
- [31] M. Kinouchi, T. Akazawa, T. Oe, R. Kogure, K. Kawabata, Y. Nakakita, *Battery separator and lithium secondary battery*. Available at <https://image-ppubs.uspto.gov/dirsearch-public/print/downloadPdf/6627346>.

- [32] J. Brito, *et al.*, *ACS Appl. Mater. Interfaces*. **2021**, *13*, 41372–41395, DOI 10.1021/acsmami.1c08061.
- [33] M. Haunschmidt, C. W. Klampfl, W. Buchberger, R. Hertsen, *Analyst* **2010**, *135*, 80–85, DOI 10.1039/b911040b.
- [34] R. Stockhausen, *et al.*, *J. Electrochem. Soc.* **2021**, *168*, 80504, DOI 10.1149/1945-7111/ac1894.
- [35] A. Smith, *et al.*, *Batteries Supercaps*. **2023**, *6*, DOI 10.1002/batt.202300080.
- [36] B. L. D. Rinkel, D. S. Hall, I. Temprano, C. P. Grey, *J. Am. Chem. Soc.* **2020**, *142*, 15058–15074, DOI 10.1021/jacs.0c06363.
- [37] F. Matsumoto, T. Gunji, *Water in Lithium-Ion Batteries Springer Nature Singapore*, Singapore, **2022**, <https://doi.org/10.1007/978-981-16-8786-0>.
- [38] R. Petibon, *et al.*, *J. Electrochem. Soc.* **2014**, *161*, A1167–A1172, DOI 10.1149/2.117406jes.
- [39] A. Hofmann, *et al.*, *Electrochimica Acta* **2022**, *403*, 139670, DOI 10.1016/j.electacta.2021.139670.
- [40] N. N. Sinha, *et al.*, *J. Electrochem. Soc.* **2011**, *158*, A1194, DOI 10.1149/2.007111jes.
- [41] S. Solchenbach, G. Hong, A. T. S. Freiberg, R. Jung, H. A. Gasteiger, *J. Electrochem. Soc.* **2018**, *165*, A3304–A3312, DOI 10.1149/2.0511814jes.
- [42] H. Shin, J. Park, A. M. Sastry, W. Lu, *J. Power Sources* **2015**, *284*, 416–427, DOI 10.1016/j.jpowsour.2015.03.039.
- [43] C. Zhan, T. Wu, J. Lu, K. D. Amine, *Energy Environ. Sci.* **2018**, *11*, 243–257, DOI 10.1039/c7ee03122j.

Manuscript received: June 7, 2024
Revised manuscript received: July 25, 2024
Accepted manuscript online: August 22, 2024
Version of record online: October 22, 2024
